the allowed linear susceptibility elements of $BaTiO_3$ in the tetragonal phase indicate that the birefringence is proportional to the square of the polarization. This is observed experimentally.[19,20] The measurements by Miller[12] of the temperature dependence of the second-harmonic susceptibility indicate that the third-rank tensor elements are linearly proportional to the polarization. A similar dependence is predicted by the theory. As for KH_2PO_4, there should exist relations between the fourth-rank tensor elements which are responsible for the birefringence and the polarization induced second-harmonic susceptibility. Hofmann[21] has recently measured the temperature dependence of the refractive index for the ordinary wave. This index does not change at the transition, indicating that the total birefringence results from a change of n_3. The above theory would then indicate that the relative values of the second-harmonic elements should differ appreciably. Miller's results indicate, however, that the nonlinear tensor elements do not differ by more than a factor 2.5.

Note added in proof. Recently J. E. Geusic, S. K. Kurtz, L. C. Van Uitert, and S. H. Wemple, [Appl. Phys. Letters 4, 141 (1964)] have measured the electro-optic properties of ABO_3 perovskites in the paraelectric phase at 6328 Å. Their values of the quadratic electro-optic tensor elements of $BaTiO_3$, expressed in terms of the static polarization, and the second-harmonic tensor elements of this crystal obtained by Miller[12] are consistent with the theory discussed here to within the experimental accuracy. They are not consistent with Hofmann's data.[21]

[19] W. J. Merz, Phys. Rev. **76**, 1221 (1949).
[20] H. F. Kay and P. Vousden, Phil. Mag. **40**, 1019 (1949).
[21] R. Hofmann, Helv. Phys. Acta **35**, 532 (1962).

PHYSICAL REVIEW VOLUME 135, NUMBER 6A 14 SEPTEMBER 1964

Linear Electric Shifts in the Nuclear Quadrupole Interaction in Al_2O_3*

R. W. DIXON AND N. BLOEMBERGEN
Division of Engineering and Applied Physics, Harvard University, Cambridge, Massachusetts
(Received 23 March 1964)

Electric perturbations of the nuclear magnetic resonances of the Al^{27} nuclei in single-crystal aluminum oxide are discussed. Splittings of the quadrupole satellite resonance lines have been obtained using fields as high as 300 kV/cm. The splittings are caused by equal and opposite changes in the electric-field gradient tensor at crystallographic aluminum sites related to each other by inversion symmetry. Magnitudes and relative signs of the five independent R-tensor elements which completely describe the electrically induced shifts for the C_3 site symmetry of the aluminum nucleus have been determined by applying electric and magnetic fields in various crystallographic directions. These data are compared with similar data obtained earlier from electric shifts in the electron spin resonances of the Cr^{3+} ion in the same cyrstal.

I. INTRODUCTION

LINEAR electrically induced changes in nuclear and electron spin resonance spectra may exist whenever the site of the interaction lacks inversion symmetry.[1] The first observation of these electrically induced effects was in pure nuclear quadrupole resonance spectroscopy,[2,3] and several more detailed investigations have since been carried out.[4–6] Electric shifts in paramagnetic resonance spectra were first investigated by Ludwig and Woodbury,[7] who worked with interstitial transition metal ion impurities in silicon. Artman and Murphy[8] observed linear shifts in the $m_s=\pm\frac{3}{2}\rightarrow\pm\frac{1}{2}$ transitions of the Cr^{3+} ion in Al_2O_3 for the special case in which the magnetic and electric fields are applied parallel to the crystallographic c axis, and subsequently, Royce and Bloembergen[9] investigated the complete tensor describing electrically induced shifts in the Cr^{3+} electron-spin resonance spectra in ruby.

Electrically induced splittings in the optical emission spectra of small concentrations of paramagnetic ions in aluminum oxide have also been investigated.[10–12]

* This paper is based on portions of a thesis presented to Harvard University in fulfillment of the thesis requirement for the Ph.D. degree and has been supported by the Joint Services through the U. S. Office of Naval Research Contract 1866(16).
[1] N. Bloembergen, Science **133**, 1363 (1961).
[2] T. Kushida and K. Saiki, Phys. Rev. Letters **7**, 9 (1961).
[3] J. Armstrong, N. Bloembergen, and D. Gill, Phys. Rev. Letters **7**, 11 (1961).
[4] J. Armstrong, N. Bloembergen, and D. Gill, J. Chem. Phys. **35**, 1132 (1961).
[5] F. A. Collins, Bull. Am. Phys. Soc. **9**, 25 (1964); thesis, Harvard University (unpublished); Phys. Rev. (to be published).
[6] R. W. Dixon, Bull. Am. Phys. Soc. **8**, 350 (1963); thesis, Harvard University (unpublished); J. Chem. Phys. (to be published).
[7] G. W. Ludwig and H. H. Woodbury, Phys. Rev. Letters **7**, 240 (1961).
[8] J. O. Artman and J. C. Murphy, Bull. Am. Phys. Soc. **7**, 14 (1962).
[9] E. B. Royce and N. Bloembergen, Phys. Rev. **131**, 1912 (1963).
[10] W. Kaiser, S. Sugano, and D. L. Wood, Phys. Rev. Letters **6**, 605 (1961).
[11] M. D. Sturge, Phys. Rev. **133**, A795 (1964).
[12] M. G. Cohen and N. Bloembergen, Bull. Am. Phys. Soc. **9**, 88, (1964). M. G. Cohen, thesis, Harvard University, 1963 (unpublished); M. G. Cohen and N. Bloembergen, Phys. Rev. (to be published).

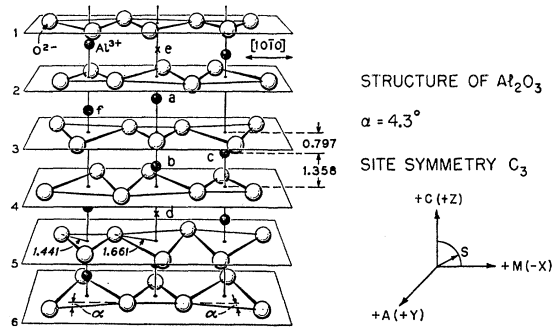

FIG. 1. Portion of the Al_2O_3 lattice showing the coordinate system used in this work. (After Geschwind and Remeika, Ref. 18.)

This paper discusses perturbations by an externally applied dc electric field of the nuclear quadrupole coupling at Al^{27} nuclei in single crystals of Al_2O_3. A preliminary report of the work was given previously.[13] The formal similarity of the development given in the next section and that used by Royce and Bloembergen[9] occurs because Cr^{3+} enters substitutionally for Al in Al_2O_3 and because the spin Hamiltonians, shown in Eqs. (1) and (2) for zero applied electric field and neglecting dipolar interactions, are formally identical.[14,15]

$$\mathcal{H}_{Cr}=g\beta\mathbf{H}_0\cdot\mathbf{S}+D[S_z^2-(S/3)(S+1)]. \quad (1)$$

$$\mathcal{H}_{Al}=-\gamma\hbar\mathbf{H}_0\cdot\mathbf{I}+(3e^2qQ/40)[I_z^2-(I/3)(I+1)]. \quad (2)$$

The similarity allows meaningful comparison of the electrically induced shifts in the two cases.

II. PHENOMENOLOGICAL THEORY

The 100% abundant Al^{27} isotope possesses nuclear spin $\frac{5}{2}$ and a quadrupole moment of 0.149 b. Pound[16] first showed that in Al_2O_3 the Zeeman energy levels of the Al^{27} nuclei are perturbed by the nuclear electric quadrupole interaction, with the result that in a single crystal there exist five NMR $\Delta m=1$ transitions in high magnetic field. These consist of a center line near the Zeeman frequency and two pairs of symmetrically placed satellites. The separation of the satellites from the central line, to first order in e^2qQ, is for the $m\rightarrow(m-1)$ transition[16]

$$\nu(m\rightarrow m-1)-\nu_Z=(3e^2qQ/20h)(m-1/2)\times(3\cos^2\theta-1)/2. \quad (3)$$

θ is the angle between the crystallographic c axis and the magnetic field. The maximum satellite splittings are 359 kc/sec for a $\frac{3}{2}\rightarrow\frac{1}{2}$ transition and 718 kc/sec for a $\frac{5}{2}\rightarrow\frac{3}{2}$ transition.

In the more general case in which an applied electric field is also present, the spin Hamiltonian given by Eq. (2) must be written

$$\mathcal{H}=-\gamma\hbar\mathbf{H}_0\cdot\mathbf{I}+\sum_{ij}[eQ/6I(2I-1)][\{\tfrac{3}{2}(I_iI_j+I_jI_i)-\delta_{ij}I(I+1)\}V_{ij}]. \quad (4)$$

V_{ij} are the components of the electric-field gradient tensor in the system of axes to which i, j pertain. Consider one kind of Al site in the unit cell and let V_{IJ} be the components of the electric-field gradient tensor in the right-hand axes system (X,Y,Z). X and Y are arbitrarily defined parallel to the $-m$ and $+a$ crystallographic directions, respectively, and Z parallel to the crystallographic c axis. The latter alone determines the quadrupole contribution to the total Hamiltonian in the absence of an external field. Then, in general,

$$V_{IJ}=V_{IJ}^0+\Delta V_{IJ}^E \text{ or}$$

$$V_{IJ}=eq_{IJ}=eq_{IJ}^0+\Sigma_K R_{KIJ}E_K, \quad (5)$$

where R_{IJK} is a third-rank tensor phenomenologically describing the linear electric shifts.[3] In the absence of applied fields $q_{IJ}^0=q_{II}^0\delta_{IJ}$; and $q_{XX}^0=q_{YY}^0=-\frac{1}{2}q_{ZZ}^0$. Introducing the description of the electric shifts through the use of the R tensor allows the restrictions imposed by site symmetry to be easily included without necessitating any approximate calculations. V_{ij} for insertion into Eq. (4), may be obtained by rotating (XYZ) into coincidence with (xyz) according to the usual formulas for rotation of a tensor of rank two.

The NMR spectrum in Al_2O_3 is a superposition of signals from nuclei at four sets of lattice sites, shown as a, b, c, and f in Fig. 1, which, in the absence of electric fields, are magnetically equivalent.[17,18] Sites a and f are related to each other by inversion symmetry, as are b and c. Sites a and c are related by reflection through the mirror plane containing the c and m axes, as are b and f. The space group is D_{3d}^6 and the site symmetry of the Al^{27} nucleus is C_3. Because the space group contains the inversion operation, the electrically induced shifts are always observed as line splittings. Lattice inversion symmetry denies the ability to assign an absolute sign to any of the R components which describe the electrically induced effects, but it does assure that no piezoelectric contribution to R is possible. The splittings are always observed at constant strain. When the

TABLE I. Independent R components in C_3 symmetry.

i \ jk	11	22	33	32 23	31 13	21 12
1	R_{111}	$-R_{111}$	0	R_{123}	R_{113}	$-R_{222}$
$R_{ijk}=2$	$-R_{222}$	R_{222}	0	R_{113}	$-R_{123}$	$-R_{111}$
3	$-\frac{1}{2}R_{333}$	$-\frac{1}{2}R_{333}$	R_{333}	0	0	0

[13] N. Bloembergen and R. W. Dixon, Bull. Am. Phys. Soc. 8, 350 (1963).
[14] G. M. Zverev and A. M. Prokhorov, Zh. Eksperim. i Teor. Fiz. 34, 513 (1958) [English transl.: Soviet Phys.—JETP 7, 354 (1958)].
[15] J. E. Geusic, Phys. Rev. 102, 1252 (1956).
[16] R. V. Pound, Phys. Rev. 79, 685 (1950).
[17] W. G. Wyckoff, *Crystal Structures* (Interscience Publishers, Inc., New York, 1960).
[18] S. Geschwind and J. P. Remeika, J. Appl. Phys. Suppl. 33, 370 (1962).

restrictions imposed by the C_3 nuclear site symmetry of Al^{27} in Al_3O_3 are introduced, the reduced R tensor has the form shown in Table I.[19] Five independent components exist in this symmetry. Note that the Voigt notation has not been used; that is no new quantities R_{11}, etc., have been defined. This avoids confusion concerning factors of two in the definition of the off-diagonal components. The trace restrictions $\sum_J R_{IJJ}=0$ have been applied with no loss in generality.

By defining the R tensor in the system of axes indicated in Fig. 1, the individual components R_{IJK} will possess the same magnitude for all four sites in the unit cell, only the sign combinations will change from one site to another. The *relative* signs of the R tensor components at the four different sites are shown in Table II, where it is assumed for reference purposes that all components at site a possess positive sign.

It now remains to determine the eigenvalues of the Hamiltonian. Eq. (4) may be expressed in the form

$$\mathcal{H}_{\text{total}}=\mathcal{H}_Z+\mathcal{H}_Q+\mathcal{H}_E, \tag{6}$$

where $\mathcal{H}_Z$ is the Zeeman Hamiltonian, $\mathcal{H}_Q$ is the quadrupole Hamiltonian in zero electric field, and $\mathcal{H}_E$ is the electric-field-dependent term in the quadrupole Hamiltonian. The orders of magnitude of the contributions to a $\Delta m=1$ frequency for typical fields used in these experiments were $\mathcal{H}_Z\cong 10$, $\mathcal{H}_Q\cong 0.4$, and $\mathcal{H}_E\cong 0.04$ Mc/sec.

Pound[16] has given a complete theory for the Hamiltonian consisting of the first two terms of Eq. (6) which agrees well with the observed Al^{27} resonant frequencies in single-crystal Al_2O_3 and their angular dependencies. The emphasis of the present discussion will be directed toward ascertaining and understanding the effects of $\mathcal{H}_E$ on the resonant frequencies. For this purpose a perturbation calculation is clearly indicated and will be carried out in two approximations. The first takes the Zeeman wave functions as zeroth-order wave functions, ignoring the existence of the initial quadrupole interaction. This approximation is expected to neglect terms of the order ν_Q/ν_Z where ν_Q measures the maximum satellite separation and ν_Z is the Zeeman frequency. In the present experiments $\nu_Q/\nu_Z\cong 4\%$. This approximation will be sufficiently accurate for most purposes.

TABLE II. Relative signs of R tensor elements for four nonequivalent lattice sites.

	Site a	Site f	Site c	Site b
R_{111}	+	−	+	−
R_{222}	+	−	−	+
R_{333}	+	−	+	−
R_{123}	+	−	−	+
R_{113}	+	−	+	−

[19] For an excellent discussion of the symmetry properties of third-rank tensors see J. F. Nye, *Physical Properties of Crystals* (Clarendon Press, Oxford, 1960).

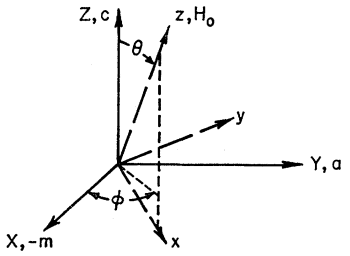

FIG. 2. System of axes used in calculating the electrically induced frequency shifts.

Corrections to it are found by considering first-order perturbations by $\mathcal{H}_E$ of wave functions formed by Zeeman states corrected in first order by the initial quadrupole interaction. This approximation will be correct to order ν_Q/ν_Z but will neglect terms of order $(\nu_Q/\nu_Z)^2\cong 0.2\%$. This is considerably less than the attainable experimental accuracy. From Eq. (4) the zero electric field quadrupole Hamiltonian may be written:

$$\mathcal{H}_Q{}^{5/2}=\sum_{jk}(eQ/60)[\tfrac{3}{2}(I_jI_k+I_kI_j)-\delta_{jk}I(I+1)]V_{jk}{}^0. \tag{7}$$

$\mathcal{H}_E$ is given by the same expression when $V_{jk}{}^0$ are replaced by $\Delta V_{jk}{}^E$, where the latter are given by

$$\Delta V_{JK}{}^E=\sum_I E_I R_{IJK}.$$

The components $V_{JK}{}^0$ and $\Delta V_{JK}{}^E$ are known in the crystallographic axes system and may be found in any other by applying the transformation

$$V_{ij}=\sum_{IJ} A_{iI}A_{jJ}V_{IJ}. \tag{8}$$

The transformation to the coordinate system in which H_0 is the z axis is given by

$$A_{iI}=\begin{pmatrix}\cos\theta\cos\varphi & \cos\theta\sin\varphi & -\sin\theta\\ -\sin\varphi & \cos\varphi & 0\\ \sin\theta\cos\varphi & \sin\theta\sin\varphi & \cos\theta\end{pmatrix}. \tag{9}$$

The angles θ and φ are defined by reference to Fig. 2 and give the direction of H_0 with respect to the crystallographic coordinate axes. The first-order frequency shifts are defined as

$$\Delta\nu_E{}^{(1)}=h^{-1}[\langle m-1|H_E|m-1\rangle-\langle m|H_E|m\rangle].$$

The indicated matrix elements are evaluated for the Hamiltonian [Eq. (7)] and give

$$\Delta\nu_E{}^{(1)}=(eQ/20h)(1-2m)\times[\Delta V_{zz}{}^E-\tfrac{1}{2}(\Delta V_{xx}{}^E+\Delta V_{yy}{}^E)]. \tag{10}$$

$\Delta V_{ii}{}^E$ are found using the tensor relations (8) and the form of the R tensor for C_3 symmetry (Table I), and the frequency shift is found to be

$$\begin{aligned}\nu(-\tfrac{3}{2}\rightarrow-\tfrac{5}{2})-\nu_Z&=(3eQ/10h)[(eq^0+E_3R_{333})(3\cos^2\theta-1)/2\\&\quad+\sin^2\theta\cos2\varphi(E_1R_{111}-E_2R_{222})\\&\quad+\sin^2\theta\sin2\varphi(-E_2R_{111}-E_1R_{222})\\&\quad+\sin2\theta\cos\varphi(E_1R_{113}-E_2R_{123})\\&\quad+\sin2\theta\sin\varphi(E_1R_{123}+E_2R_{113})].\end{aligned} \tag{11}$$

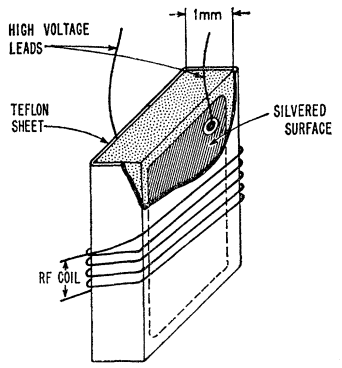

FIG. 3. Detail of Al_2O_3 sample showing method of applying electric field.

Eq. (11) gives the frequency shift of the $-\frac{3}{2}\rightarrow-\frac{5}{2}$ transition, in the presence of an electric field $\mathbf{E}=(E_1,E_2,E_3)$ in the crystallographic axes system, for one kind of Al site, neglecting terms of order (ν_Q/ν_Z) and higher.

The correction to Eq. (11) to second-order perturbation, using $\mathcal{H}_Q$ and $\mathcal{H}_E$ once each, is

$$\Delta\nu_E^{(2)}=(eQ/30h)(\nu_Q/\nu_Z)[-24\Delta V_{xz}{}^E\sin2\theta -\tfrac{3}{2}(\Delta V_{xx}{}^E-\Delta V_{yy}{}^E)\sin^2\theta]. \quad (12)$$

$\Delta V_{ij}{}^E$ may be calculated as before, and the discussion restricted to the three special cases which suffice for present purposes, namely those for which $\varphi=0$, $\mathbf{E}=(E_1,0,0)$; $\varphi=0$, $\mathbf{E}=(0,E_2,0)$; and $\theta=0$, $\mathbf{E}=(0,0,E_3)$. In the latter case Eq. (12) shows that $\Delta\nu_E{}^{(2)}$ is zero, and R_{333} is given correct to terms in $(\nu_Q/\nu_Z)^2$ by $\Delta\nu_E{}^{(1)}$. Actually, because $|m\rangle$ are eigenstates of both $\mathcal{H}_Z$ and $\mathcal{H}_Q$ for this direction of the magnetic field, R_{333} is given correctly by $\Delta\nu^{(1)}$ to all orders of (ν_Q/ν_Z), only terms in E^2 being neglected. In the remaining two cases, in an approximation which affects computed values of R_{ijk} by less than 1%.

$$\Delta\nu^{(2)}[\varphi=0,\ \mathbf{E}=(E_1,0,0)] =(3eQ/10h)(\nu_Q/\nu_Z)(-4E_1/3) \times(R_{111}\sin^2\!2\theta+R_{113}\sin4\theta), \quad (13a)$$

$$\Delta\nu^{(2)}[\varphi=0,\ \mathbf{E}=(0,E_2,0)] =(3eQ/10h)(\nu_Q/\nu_Z)(4E_2/3) \times(R_{222}\sin^2\!2\theta+R_{123}\sin4\theta). \quad (13b)$$

It is now clear that $\Delta\nu_E{}^{(1)}$ is a sufficiently accurate expression to yield values of R_{111} and R_{222} to within 1% ($\theta=\pi/2$ for their measurement). Thus $\Delta\nu_E{}^{(2)}$ will be a correction only for the computation of R_{113} and R_{123} from the experimental data, where the corrections are 15 and 10%, respectively. Such corrections are of the order of the experimental error for these components.

III. EXPERIMENTAL PROCEDURE AND RESULTS

Combining the information in Eq. (11) and Table II it is possible, by judiciously choosing the directions of the electric and magnetic fields, to design experiments which will in theory permit the determination of all five R components and their relative signs. Table II must be used to insure that the $-\frac{3}{2}\rightarrow-\frac{5}{2}$ transition splits into two lines, rather than into four, as it would in general. (The inversion symmetry of the lattice requires, in either case, that the splitting be symmetric about the unsplit line.) This simplifies the analysis of data in those cases in which only a broadening of the resonance line can be detected in the strongest available electric fields.

The following experiments were performed:

(1) $\mathbf{E}=(0,0,E_3)$; $\mathbf{H}_0$ parallel to c. Then

$$\nu(-\tfrac{3}{2}\rightarrow-\tfrac{5}{2})-\nu_Z=(3eQ/10h)(eq^0\pm R_{333}E_3)$$

and R_{333} is measured.

(2) $\mathbf{E}=(E_1,0,0)$; $\mathbf{H}_0$ in the XY plane. Then

$$\nu(-\tfrac{3}{2}\rightarrow-\tfrac{5}{2})-\nu_Z=(3eQ/10)[-\tfrac{1}{2}eq^0 \pm(\cos2\varphi R_{111}\mp\sin2\varphi R_{222})E_1]$$

and R_{111} is measured for $\varphi=0$ and R_{222} is measured for $\varphi=\pm\pi/4$.

(3) $\mathbf{E}=(E_1,0,0)$; $\mathbf{H}_0$ in the XZ plane. Then

$$\nu(-\tfrac{3}{2}\rightarrow-\tfrac{5}{2})-\nu_Z=(3eQ/10h)[eq^0(3\cos^2\theta-1)/2 \pm(R_{111}\sin^2\theta+R_{113}\sin2\theta)E_1]$$

and R_{111} is measured for $\theta=\pi/2$ and the magnitude and relative sign of R_{113} are measured for $\theta=\pi/4$ and $3\pi/4$.

(4) $\mathbf{E}=(0,E_2,0)$; $\mathbf{H}_0$ in the XZ plane. Then

$$\nu(-\tfrac{3}{2}\rightarrow-\tfrac{5}{2})-\nu_Z=(3eQ/10h)[eq^0(3\cos^2\theta-1)/2 \pm(R_{222}\sin^2\theta+R_{123}\sin2\theta)E_2]$$

and R_{222} is measured for $\theta=\pi/2$ and the magnitude and relative sign of R_{123} are obtained for $\theta=\pm\pi/4$.

(5) $\mathbf{E}=(\sqrt{3}/2,0,\frac{1}{2})E_0$; $\mathbf{H}_0$ in the XZ plane. Then

$$\nu(-\tfrac{3}{2}\rightarrow-\tfrac{5}{2})-\nu_Z=(3eQ/10h)[\{eq_0\pm\tfrac{1}{2}R_{333}\} \times(3\cos^2\theta-1)/2\pm\tfrac{3}{2}(\sin^2\theta R_{111}+\sin2\theta R_{113})E_0]$$

and the relative sign of R_{111} and R_{333} is obtained for $\theta=\pi/2$. This set of experiments determines relative signs between R_{111}, R_{113}, and R_{333}; and between R_{123}

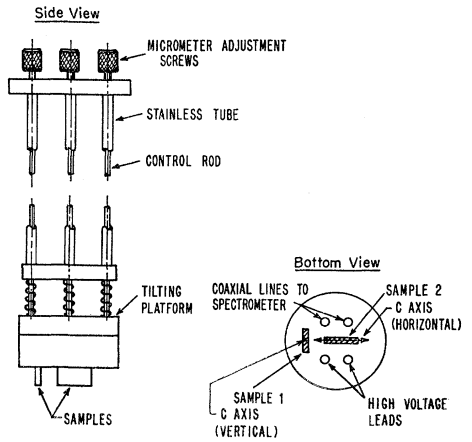

FIG. 4. Tiltable sample holder used to align samples in the magnetic field.

and R_{222}. The symmetries of the four kinds of sites with respect to each other determine the relative sign between these two groups of components, but deny the possibility of assigning an absolute sign to any component.

All experimental measurements were performed on $\alpha-Al_2O_3$ containing 0.05% Cr^{3+} (obtained from the Linde Company). The Cr^{3+} shortens the longitudinal relaxation time to more convenient values than are available in pure Al_2O_3.[20] R_{333} was also measured in pure Al_2O_3 and in Al_2O_3: 0.5% Cr^{3+}, the results being identical with the measurement in Al_2O_3: 0.05% Cr^{3+}.

Figure 3 indicates the sample geometry. The coil wrapped around the assembly was made the tank circuit of a standard radio-frequency spectrometer.[21] Note that $\mathbf{H}_{rf}$ and $\mathbf{E}_0$ are always perpendicular. Two layers of 0.005-in. Teflon sheet served to insulate the coil from the high-voltage electrodes. Since voltages as high as 30 000 V were applied across 1-mm-thick samples, care was necessary to prevent electrical breakdown from occurring between the two sample electrodes or between one of the electrodes and the surroundings. Flexrock No. 80 cement proved to be a useful insulating material. Experiments were normally performed at 77°K, where emersion of the sample in liquid nitrogen also had a desirable insulating effect. Sample electrodes were formed using Dupont No. 7713 silver-bearing paint, and high-voltage leads were attached using ordinary solder. Typical sample size was 1 cm×1 cm×1 mm. Electric fields were applied using voltages obtained from either a stack of dry cells (up to 10 000 V) or from a Del electronic dc power supply (up to 30 000 V).

Samples could be oriented for cutting using x-ray back reflection Laue techniques to accuracies of $\pm\frac{1}{2}$ deg. By mounting two similar samples with c axes accurately at right angles to each other in a tiltable sample holder, the variation of satellite separation as a function of

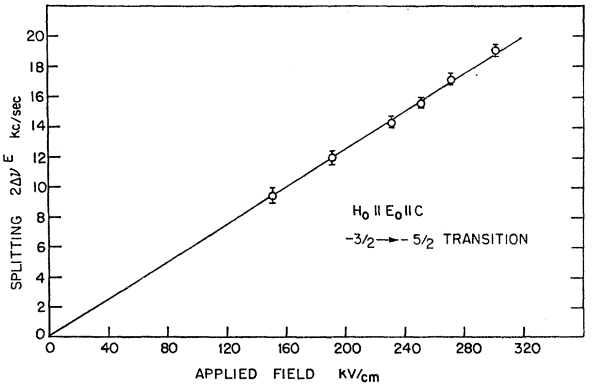

FIG. 5. Magnitude of the electrically induced splitting of the $-\frac{3}{2} \rightarrow -\frac{5}{2}$ transition of the Al^{27} nuclear magnetic resonance in $\alpha-Al_2O_3$.

[20] C. M. Verber, M. P. Mahon, and W. H. Tantilla, Phys. Rev. 125, 1149 (1962).
[21] G. D. Watkins and R. V. Pound, Phys. Rev. 82, 343 (1951).

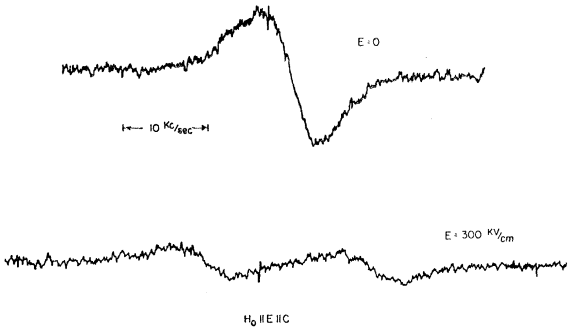

FIG. 6. Experimental tracing of the electrically induced splitting of the $\frac{5}{2} \rightarrow \frac{3}{2}$ transition from Al^{27} nuclei in Al_2O_3.

magnetic field direction could be used to completely orient the sample in the magnetic field. A sketch of the holder is shown in Fig. 4. The magnetic field could be rotated in the horizontal plane.

Figure 5 shows the values of splitting versus electric field for the $-\frac{3}{2} \rightarrow -\frac{5}{2}$ transition when $\mathbf{E}$ and $\mathbf{H}$ are parallel to the c axis. Note that the linearity of the splitting as a function of electric field is experimentally confirmed. A typical experimental splitting of the absorption derivative for this geometry and 300 000 V/cm is shown in Fig. 6. The splitting is symmetric about the unsplit line. The value of R_{333} so measured is larger than the other components of R, and it was felt that the known value of R_{333} could be combined with the low-field experimental curves to construct an empirical relation between line broadening and splitting. This relation was then used in the evaluation of the data for the R components R_{111}, R_{123}, and R_{113} where enough field could not be applied to clearly split the resonance line. The procedure follows that used by Royce and Bloembergen.[9] A relation

$$\frac{\Delta\nu_{\min}{}^{\max}(E)}{\Delta\nu_{\min}{}^{\max}(0)} = K\left[\frac{2\Delta\nu_E(E)}{\Delta\nu_{\min}{}^{\max}(0)}\right]^2 \qquad (12)$$

was assumed, and found to hold well for the low-field values used to measure R_{333}. $\Delta\nu_{\min}{}^{\max}$ is the linewidth between maximum and minimum of the absorption derivative and $2\Delta\nu_E$ is the (unresolved) splitting of the two lines. K was determined to be equal to 0.98. This relation must be viewed as approximate because of the unsymmetric line shape of the Al^{27} nuclear resonance in Al_2O_3,[22] but is considered adequate within the quoted error. All measurements indicated in the five experiments outlined above were repeated on at least two samples, and the resulting experimental values of R components for two kinds of sites are shown in Table III. The other two kinds of sites have all signs reversed. For completeness a $\frac{3}{2} \rightarrow \frac{1}{2}$ transition was also monitored at 300 kV/cm with $\mathbf{E}$ and $\mathbf{H}_0$ parallel to the c axis and

[22] A. H. Silver, T. Kushida, and J. Lambe, Phys. Rev. 125, 1147 (1962).

TABLE III. Experimental values of R tensor elements (in 10^9 cm^{-1}) for Al^{27} electric shifts.

Component	Site 1[a]	Site 2[a]
R_{333}	−2.9	−2.9
R_{222}	1.55	−1.55
R_{111}	1.1	1.1
R_{113}	0.4	0.4
R_{123}	−0.7	0.7

[a] All uncertainties are $\pm 0.1 \times 10^9$ cm^{-1}; other two kinds of sites have all signs reversed.

the splitting found to be one-half of that of the $\frac{5}{2} \rightarrow \frac{3}{2}$ line. No electric field shifts in the $-\frac{1}{2} \rightarrow \frac{1}{2}$ transition could be detected for this configuration and 300 kV/cm applied field. Both of these results are consistent with the phenomenological theory.

IV. COMPARISON OF RESULTS WITH CHROMIUM ELECTRIC SHIFTS

Equation (1) gives the Hamiltonian describing Cr^{3+} electron spin resonance in Al_2O_3. The effective spin is $\frac{3}{2}$, and $2D$ has the value 11.46 kMc/sec. Royce and Bloembergen describe the electrically induced shifts in the electron spin resonance spectrum through the addition of another term in the Hamiltonian, viz.:

$$\mathcal{H}_E = \sum_i \sum_{j>k} R_{ijk}^{Cr} \{ (S_j S_k + S_k S_j)/2 \} E_i. \qquad (13)$$

Their experimental values for R_{ijk}^{Cr} are shown in Table IV. Care is necessary in comparing the two sets of R components because of differences in their definitions. R_{333}^{Cr} and R_{333}^{Al} are compared by forming the ratios $(\Delta q/q_0)^{Al}$ and $(\Delta D/D)^{Cr}$, that is by comparing the relative induced field gradient in the c direction to the relative induced crystal field splitting in the c direction. The values are

$$(\Delta D/D) = (4.67 \pm 0.09) \times 10^{-3} \text{ per } 100 \text{ kV/cm},$$
$$(\Delta q/q_0) = (4.37 \pm 0.15) \times 10^{-3} \text{ per } 100 \text{ kV/cm}.$$

This near equality of the relative variations can be understood on the basis that ionic displacements from a perfect octahedral arrangement play the same role in both cases. However, the effects cannot be ascribed solely to a displacement of point charges. In that case the ratio of all elements in the R tensor for Al^{27} should be the same as the corresponding ratios for Cr^{3+}. Experimental results show that this is far from the truth. Define $g_{ijk}^{Al} \equiv R_{ijk}^{Al}/R_{333}^{Al}$ and $g_{ijk}^{Cr} \equiv R_{ijk}^{Cr}/R_{333}^{Cr}$; except that g_{113}^{Al} and g_{123}^{Al} are twice the indicated quantities to take account of differences in the definitions of R^{Al} and R^{Cr}. Then

$$g_{111}^{Al} = 0.38 \pm 0.03, \qquad g_{111}^{Cr} = 0.11 \pm 0.02,$$
$$g_{222}^{Al} = 0.54 \pm 0.03, \qquad g_{222}^{Cr} = 0.41 \pm 0.02,$$
$$g_{113}^{Al} = 0.28 \pm 0.06, \qquad g_{113}^{Cr} = 0.50 \pm 0.1,$$
$$g_{123}^{Al} = 0.48 \pm 0.06, \qquad g_{123}^{Cr} = 0.22 \pm 0.1.$$

Magnitudes of the ratios of these quantities are

$$g_{111}^{Al}/g_{111}^{Cr} = 3.45 \pm 0.7,$$
$$g_{222}^{Al}/g_{222}^{Cr} = 1.32 \pm 0.09,$$
$$g_{113}^{Al}/g_{113}^{Cr} = 0.56 \pm 0.15,$$
$$g_{123}^{Al}/g_{123}^{Cr} = 2.2 \pm 1.1.$$

The magnitudes show serious departures from unity. Agreement is even worse when the signs are compared. The experimental results show that for all sites in the unit cell $R_{113}^{Al}/R_{333}^{Al}$ and $R_{113}^{Cr}/R_{333}^{Cr}$ have opposite sign, as do $R_{123}^{Al}/R_{222}^{Al}$ and $R_{123}^{Cr}/R_{222}^{Cr}$. $R_{111}^{Al}/R_{333}^{Al}$ and $R_{111}^{Cr}/R_{333}^{Cr}$ have the same sign. Note again that neither the experiments of Royce and Bloembergen nor those discussed here are capable of assigning a particular set of R_{ijk} (with proper signs) to a particular site (a, b, c, or f) in the unit cell. Therefore nothing more can be said about the sign of $R_{ijk}^{Al}/R_{ijk}^{Cr}$ for a particular lattice site. One consistent choice is $R_{333}^{Al}/R_{333}^{Cr}$, $R_{111}^{Al}/R_{111}^{Cr}$, and $R_{222}^{Al}/R_{222}^{Cr}$ positive, but $R_{113}^{Al}/R_{113}^{Cr}$ and $R_{123}^{Al}/R_{123}^{Cr}$ negative. Three other possibilities clearly exist.

Royce and Bloembergen have applied detailed microscopic calculations of Lohr and Lipscomb[23] to the problem of the electric shifts of the paramagnetic resonance of Cr^{3+}. These calculations show that the ionic displacements induced by the applied electric field act indirectly on the splitting by changing the residual covalency of the orbitals in the CrO_6 complex. A similar calculation has not been carried out for the AlO_6 complex but should be quite interesting. Since, in the absence of an applied electric field, the field gradient tensor has axial symmetry, there is no calibration for the change in gradient due to transverse ionic displacements. The model, in which ionic displacements around the complex cause changes in the partial covalency of the electronic orbitals, can thus account both for the equality $\Delta D/D = \Delta q/q_0$ and for the absence of proportionality between the two R tensors. Although for many purposes Al_2O_3 may be considered as an ionic solid, the polarization of partial covalent orbitals is probably very important in determining the magnitudes of the

TABLE IV. Experimental values of R tensor elements for chromium electric shifts.[a]

Component	Site 1[b]	Site 2[b]
R_{111}	−(0.020±0.003)	−(0.020±0.003)
R_{222}	(0.073±0.003)	−(0.073±0.003)
R_{333}	(0.179±0.003)	(0.179±0.003)
R_{123}	(0.04±0.02)	−(0.04±0.02)
R_{113}	(0.09±0.02)	(0.09±0.02)

[a] After E. B. Royce and N. Bloembergen, Phys. Rev. **131**, 1912 (1963).
[b] Sites related by inversion symmetry have all signs reversed. The units are Mc/sec per kV/cm.

[23] L. L. Lohr, Jr., and W. N. Lipscomb, J. Chem. Phys. **38**, 1607 (1963).

R-tensor components discussed here. Such a view is supported also by an attempt to estimate the magnitude of the ionic contribution to R_{333}. This estimate (using ionic displacements calculated from the ionic contribution to the dc dielectric constant[3]) indicates that the direct ionic contribution can account for only about 20% of the magnitude of R_{333}.

V. INDUCED ASYMMETRY PARAMETER

Kushida and Silver[24] have recently observed electrically induced nuclear transitions between Al^{27} energy levels in ruby in high magnetic field. Using a Pound-Watkins spectrometer they monitored the signal intensity of a $\Delta m=1$ transition (e.g., $-\frac{1}{2}\rightarrow\frac{1}{2}$) while applying an rf *electric* field to the sample at a $\Delta m=2$ transition (e.g., $\frac{3}{2}\rightarrow-\frac{1}{2}$). The change in amplitude of the $\Delta m=1$ signal intensity as a function of rf electric-field amplitude allowed them to deduce a transition probability for electrically induced transitions. Variation of this transition probability with the square of the electric field, consistent with theory, was experimentally verified. If the quadrupole Hamiltonian is written

$$\mathcal{H}_Q=(e^2qQ/40)[3I_z^2-I(I+1)+(\eta/2)(I_+^2+I_-^2)], \quad (14)$$

an *induced* asymmetry parameter is defined which may be related to the transition probability for electrically induced transitions. The value of η_{induced} measured by Kushida and Silver is 1.5×10^{-7} $(\text{V/cm})^{-1}$.

An induced asymmetry parameter can also be computed from the dc experiments described above. Consider a dc electric field applied in the XY plane at angle ξ from the X axis ($-m$ crystallographic direction). Then $\mathbf{E}=E_0(\cos\xi, \sin\xi, 0)$, and by definition

$$\eta_{\text{induced}}=(q_{XX}{}^P-q_{YY}{}^P)/q_{ZZ}{}^P,$$

where $q_{II}{}^P$ are principal axes components. In the absence of an electric field $q_{XX}{}^P=q_{YY}{}^P=-\frac{1}{2}q_{ZZ}{}^P$ and $\eta=0$. This is required by the C_3 symmetry of the Al^{27} nucleus and is confirmed experimentally. To deduce the value of η_{induced} when an electric field is applied, $q_{II}{}^P$ must be expressed in terms of R_{ijk}, E_0, and ξ. The $q_{II}{}^P$'s are eigenvalues of the determinant (q_{ij}). Call them λ_i. Then

$$\begin{vmatrix} q_{xx}-\lambda & q_{xy} & q_{xz} \\ q_{yx} & q_{yy}-\lambda & q_{yz} \\ q_{zx} & q_{zy} & q_{zz}-\lambda \end{vmatrix}=0. \quad (15)$$

Define

$$\lambda_i=q_{ii}{}^0+\epsilon_i,$$
$$q_{ij}=q_{ij}{}^0+\Delta q_{ij}{}^E. \quad (16)$$

Substituting Eq. (16) into (15), expanding, and keeping lowest order terms in ϵ_i gives

$$|\epsilon_1|=|\epsilon_2|=[(\Delta q_{xy}{}^E)^2-(\Delta q_{xx}{}^E)(\Delta q_{yy}{}^E)]^{1/2}.$$

Thus the originally degenerate eigenvalues become $\lambda=q_{xx}{}^0\pm|\epsilon|$, which implies $|q_{XX}{}^P-q_{YY}{}^P|=2|\epsilon|$. From Eq. (5) and Table I it follows that

$$\Delta q_{xx}{}^E=-\Delta q_{yy}{}^E=(E_0/e)(R_{111}\cos\xi-R_{222}\sin\xi),$$
$$\Delta q_{xy}{}^E=-(E_0/e)(R_{222}\cos\xi+R_{111}\sin\xi).$$

Using these relations and the definition of the asymmetry parameter gives the following expression for the induced asymmetry parameter:

$$\eta_{\text{induced}}=2E_0(R_{111}{}^2+R_{222}{}^2)^{1/2}/eq_{zz}{}^0. \quad (17)$$

A most interesting feature of Eq. (17) is that it does not depend on the direction of the electric field in the XY plane. This result can be shown to be true for any axial symmetry. Substituting experimental values for R_{111}, R_{222}, and $q_{zz}{}^0$ into Eq. (17) gives

$$\eta_{\text{induced}}=(5.7\pm0.4)\times10^{-8}\ (\text{V/cm})^{-1}.$$

This is a factor 2.5 smaller than the value measured by Kushida and Silver. The present measurement is considered to be more accurate because absolute rf intensity measurements are usually less precise than dc measurements.

Directions of the principal axes of the electric field gradient tensor in the XY plane become well defined when the dc electric field is applied and may be found by considering the portion of Eq. (10) which pertains to the XY plane. The X principal axis direction is most easily expressed in terms of the vector $\mathbf{R}=(R_{111}, -R_{222}, 0)$. If $\mathbf{E}_0$ makes an angle β with $\mathbf{R}$, then $q_{XX}{}^P$ makes an angle α with X, where $\alpha=\beta/2$. Thus, it is interesting to note that although the magnitude of the induced asymmetry parameter is independent of the direction of the electric field relative to the crystallographic axes, the directions of the principal axes of the quadrupole tensor do depend on the direction of the electric field.

VI. CONCLUSION

Electric shifts in nuclear magnetic resonance provide new experimental parameters which are very sensitive to the local environment. They provide a detailed check on the accuracy of bonding orbitals and structural models of the lattice.

ACKNOWLEDGMENTS

Conversations with Dr. E. B. Royce and with Dr. F. A. Collins have been very fruitful and are gratefully acknowledged.

[24] T. Kushida and A. H. Silver, Phys. Rev. **130**, 1692 (1963).